Probing new physics in semileptonic Σ_b and Ω_b decays

Jin-Huan Sheng,[1,*] Jie Zhu,[1] Xiao-Nan Li,[1] Quan-Yi Hu,[1] and Ru-Min Wang[2,†]

[1]*School of Physics and Electrical Engineering, Anyang Normal University, Anyang, Henan 455000, China*

[2]*College of Physics and Communication Electronic, Jiangxi Normal University, Nanchang, Jiangxi 330022, China*

(Received 22 July 2020; accepted 7 September 2020; published 30 September 2020)

Recently, several hints of lepton nonuniversality have been observed in the semileptonic B meson decays in terms of both in the neutral current ($b \to s l\bar{l}$) and charged current ($b \to c l\bar{\nu}_l$) transitions. Motivated by these inspiring results, we perform the analysis of the baryon decays $\Sigma_b \to \Sigma_c l\bar{\nu}_l$ and $\Omega_b \to \Omega_c l\bar{\nu}_l (l = e, \mu, \tau)$ which are mediated by $b \to c l\bar{\nu}_l$ transitions at the quark level, to scrutinize the nature of new physics (NP) in the model independent method. We first use the experimental measurements of $\mathcal{B}(B \to D^{(*)} l\bar{\nu}_l)$, $\mathrm{R}_{D^{(*)}}$ and $\mathrm{R}_{J/\psi}$ to constrain the NP coupling parameters in a variety of scenarios. Using the constrained NP coupling parameters, we report numerical results on various observables related to the processes $\Sigma_b \to \Sigma_c l\bar{\nu}_l$ and $\Omega_b \to \Omega_c l\bar{\nu}_l$, such as the branching ratios, the ratio of branching fractions, the lepton side forward-backward asymmetries, the hadron and lepton longitudinal polarization asymmetries and the convexity parameter. We also provide the q^2 dependency of these observables and we hope that the corresponding numerical results in this work will be testified by future experiments.

DOI: 10.1103/PhysRevD.102.055023

I. INTRODUCTION

Though the Standard Model (SM) is considered as the most fundamental and successful theory which describe almost all the phenomena of the particle physics, there are still some open issues that are not discussed in the SM, like matter-antimatter asymmetry, dark matter, etc. Although there is no direct evidence for new physics (NP) beyond the SM has been found, some possible hints of NP have been observed in the B meson decay processes [1–4]. Even though the SM gauge interactions are lepton flavor universal, the hints of lepton flavor universal violation (LFUV) have also been observed in several anomalies relative to the semileptonic B meson decays. The most basic experimental measurements which substantiate these anomalies are the ratio of the branching ratios $\mathrm{R}_{D^{(*)}}$ for $b \to c l\bar{\nu}_l$ decay processes. The ratio which is defined as $\mathrm{R}_{D^{(*)}} = \frac{\mathcal{B}(B \to D^{(*)}\tau\bar{\nu}_\tau)}{\mathcal{B}(B \to D^{(*)}\ell\bar{\nu}_\ell)}$ with $\ell = e,\ \mu$ has been measured first by *BABAR* [5]. Besides Belle and LHCb also reported their results [6–10]. The experimental measurement results for these anomalies show that there is large deviations with their corresponding SM predictions. Very recently, the Belle Collaborations announced the latest measurements of $\mathrm{R}_{D^{(*)}}$ [11]

$$\mathrm{R}_D^{\mathrm{Belle}} = 0.307 \pm 0.037 \pm 0.016,$$
$$\mathrm{R}_{D^*}^{\mathrm{Belle}} = 0.283 \pm 0.017 \pm 0.014, \tag{1}$$

which are in agreement with their SM predictions about within 0.2σ and 1.1σ, respectively, and their combination agrees with the SM predictions within 1.2σ. Although the tension between the latest measurement results and their SM predictions is obviously reduced, there is still 3.08σ corresponding SM predictions on combining all measurements in the global average fields. The latest averaged results reported by Heavy Flavor Averaging Group (HFAG) are [12]

$$\mathrm{R}_D^{\mathrm{avg}} = 0.340 \pm 0.027 \pm 0.013,$$
$$\mathrm{R}_{D^*}^{\mathrm{avg}} = 0.295 \pm 0.011 \pm 0.008, \tag{2}$$

comparing with the SM predictions of $\mathrm{R}_{D^{(*)}}$ [12]

$$\mathrm{R}_D^{\mathrm{SM}} = 0.299 \pm 0.003, \qquad \mathrm{R}_{D^*}^{\mathrm{SM}} = 0.258 \pm 0.005. \tag{3}$$

One can see that above averaged experimental measurement results deviate from their SM predictions at 1.4σ and 2.5σ level, respectively.

Apart from R_D and R_{D^*} measurements, the ratio $\mathrm{R}_{J/\psi}$ has also been measured by LHCb [13]

*jinhuanphy@aynu.edu.cn
†ruminwang@sina.com

$$\mathrm{R}_{J/\psi} = \frac{\mathcal{B}(B_c \to J/\psi \tau \bar{\nu}_\tau)}{\mathcal{B}(B_c \to J/\psi l \bar{\nu}_l)} = 0.71 \pm 0.17 \pm 0.18, \quad (4)$$

which central value prediction of the SM is in the range $0.25 \sim 0.28$ and the experimental result has about 2σ tension with its SM prediction [14,15]. The uncertainties arise from the choice of the approach for the $B_c \to J/\psi$ from factors [15–18].

These deviations between the experimental measurements and their SM predictions are perhaps from the uncertainties of hadronic transition form factors. This may imply the lepton flavor universality is violated, which is the hint of the existence of NP. Many works have been done based on the model independent framework [19–25] or specific NP models by introducing new particles such as leptoquarks [26–28], SUSY particles [29,30], charged Higgses [31–33], or new vector bosons [34].

It is also important and interesting to investigate the semileptonic baryon decays $\Sigma_b \to \Sigma_c l \bar{\nu}_l$ and $\Omega_b \to \Omega_c l \bar{\nu}_l$ which are mediated by the $b \to c l \bar{\nu}_l$ transition at the quark level. Studying these processes not only can provide an independent determination of the Cabibbo-Kobayashi-Maskawa (CKM) matrix element $|V_{cb}|$, but also can confirm the LFUV in $\mathrm{R}_{\Sigma_c(\Omega_c)}$ which have a similar formalism to $\mathrm{R}_{D^{(*)}}$. We will explore the NP effects on various observables for the $\Sigma_b \to \Sigma_c l \bar{\nu}_l$ and $\Omega_b \to \Omega_c l \bar{\nu}_l$ decays in the model independent effective field theory formalism. It is necessary to study these decay modes both theoretically and experimentally to test the LFUV. There will be several difficulties to measure the branching ratio $\mathcal{B}(\Sigma_b \to \Sigma_c l \bar{\nu}_l)$ because Σ_b decay strongly and their branching ratios will be very small [35]. Nevertheless it is feasible to measure $\mathcal{B}(\Omega_b \to \Omega_c l \bar{\nu}_l)$ as Ω_b decays predominantly weakly and the branching ratio is significantly large. So it is worthwhile to study these decay processes because they can provide very comprehensive information about possible NP.

It will draw very interesting results to investigate the implications of $\mathrm{R}_{D^{(*)}}$ on the processes $\Omega_b \to \Omega_c l \bar{\nu}_l$ and $\Sigma_b \to \Sigma_c l \bar{\nu}_l$. The authors of Refs. [36–43] give the total decay rate Γ (in units of 10^{10} s^{-1}) from 1.44 to 4.3 for $\Sigma_b \to \Sigma_c e \bar{\nu}_e$ and from 1.29 to 5.4 for $\Omega_b \to \Omega_c e \bar{\nu}_e$. It is worthwhile to note that the complexity of the baryon structures and the lack of precise predictions of various form factors may lead to the variations in the prediction of the total decay rate Γ. In this paper we will give the predictions of various observables within SM and different NP scenarios. Using the NP coupling parameters constrained from the latest experimental limits from $\mathcal{B}(B \to D^{(*)} l \bar{\nu}_l)$, $\mathrm{R}_{D^{(*)}}$ and $\mathrm{R}_{J/\psi}$, we investigate the NP effects of these anomalies on the differential branching fraction $d\mathcal{B}/dq^2$, the ratios of branching fractions $\mathrm{R}_{\Omega_c(\Sigma_c)}(q^2)$, the lepton side forward-backward asymmetries $A_{FB}(q^2)$, the longitudinal polarizations $P_L^{\Sigma_c(\Omega_c)}(q^2)$ of the daughter baryons $\Sigma_c(\Omega_c)$, the longitudinal polarizations $P_L^l(q^2)$ of the lepton l and the convexity parameter $C_F^l(q^2)$. Note that there is different between our study and the Ref. [44], in which $\Omega_b \to \Omega_c l \bar{\nu}_l$ and $\Sigma_b \to \Sigma_c l \bar{\nu}_l$ have also been investigated in a model independent way. In our work the NP coupling parameters are assumed to be complex and we consider the constraints on the NP coupling parameters from the experimental limits of $\mathcal{B}(B \to D^{(*)} l \bar{\nu}_l)$, $\mathrm{R}_{J/\psi}$ and $\mathrm{R}_{D^{(*)}}$. However, NP coupling parameters are set to real and only $\mathrm{R}_{D^{(*)}}$ is considered in Ref. [44].

Our paper is organized as follows. In Sec. II we briefly introduce the effective theory describing the $b \to c l \bar{\nu}_l$ transitions as well as the form factors, the helicity amplitudes and some observables of the processes $\Omega_b \to \Omega_c l \bar{\nu}_l$ and $\Sigma_b \to \Sigma_c l \bar{\nu}_l$. Section III is devoted to the numerical results and discussions for the predictions within the SM and various NP scenarios. Our conclusions are given in Sec. IV.

II. THEORY FRAMEWORK

The most general effective Lagrangian including both the SM and the NP contribution for $B_1 \to B_2 l \bar{\nu}_l$ decay processes, where $B_1 = \Sigma_b(\Omega_b)$, $B_2 = \Sigma_c(\Omega_c)$, mediated by the quark level transition $b \to c l \bar{\nu}_l$ is given by [45,46]

$$\begin{aligned}\mathcal{L}_{\mathrm{eff}} = -\frac{4G_F}{\sqrt{2}} V_{cb} \{ & (1+V_L)\bar{l}_L \gamma_\mu \nu_L \bar{q}_L \gamma^\mu b_L \\ & + V_R \bar{l}_L \gamma_\mu \nu_L \bar{q}_R \gamma^\mu b_R + S_L \bar{l}_R \nu_L \bar{q}_R b_L \\ & + S_R \bar{l}_R \nu_L \bar{q}_L b_R + T_L \bar{l}_R \sigma_{\mu\nu} \nu_L \bar{q}_R \sigma^{\mu\nu} b_L \} + \mathrm{H.c.}, \quad (5)\end{aligned}$$

where G_F is the Fermi constant, V_{cb} is the CKM matrix elements and $(q, b, l, \nu)_{L,R} = P_{L,R}(q, b, l, \nu)$ are the chiral quark (lepton) fields with $P_{L,R} = (1 \mp \gamma_5)/2$ as the projection operators. Here we note that the NP coupling parameters $V_{L,R}$, $S_{L,R}$, T_L characterizing the NP contributions coming from the new vector, scalar, and tensor interactions are associated with left handed neutrino and these NP coupling parameters are all zero in the SM. In our work we focus on a study of the vector and scalar type interactions, excepting the tensor interaction, and we assume that the NP coupling parameters $V_{L,R}$ and $S_{L,R}$ are complex.

A. Form factors and helicity amplitudes

The hadronic matrix elements of vector and axial vector currents for the decays $B_1 \to B_2 l \bar{\nu}_l$ are parametrized in terms of various hadronic form factors as follows:

$$\begin{aligned} M_\mu^V &= \langle B_2, \lambda_2 | \bar{c} \gamma_\mu b | B_1, \lambda_1 \rangle \\ &= \bar{u}_2(p_2, \lambda_2)[f_1(q^2)\gamma_\mu + i f_2(q^2)\sigma_{\mu\nu}q^\nu + f_3(q^2)q_\mu] \\ &\quad \times u_1(p_1, \lambda_1), \\ M_\mu^A &= \langle B_2, \lambda_2 | \bar{c} \gamma_\mu \gamma_5 b | B_1, \lambda_1 \rangle \\ &= \bar{u}_2(p_2, \lambda_2)[g_1(q^2)\gamma_\mu + i g_2(q^2)\sigma_{\mu\nu}q^\nu + g_3(q^2)q_\mu]\gamma_5 \\ &\quad \times u_1(p_1, \lambda_1), \end{aligned}$$

where $\sigma_{\mu\nu} = \frac{i}{2}(\gamma_\mu\gamma_\nu - \gamma_\nu\gamma_\mu)$, $q_\mu = (p_1 - p_2)_\mu$ is the four momentum transfer. λ_1 and λ_2 are the helicities of the parent baryon B_1 and daughter baryon B_2, respectively. Here B_1 represents the bottomed baryon Σ_b or Ω_b and B_2 represents the charmed baryon Σ_c or Ω_c. Using the equation of motion, we can obtain the hadronic matrix elements of the scalar and pseudoscalar currents between these two baryons. The expressions for them can be written

$$\begin{aligned}
&\langle B_2,\lambda_2|\bar{c}b|B_1,\lambda_1\rangle = \bar{u}_2(p_2,\lambda_2)\\
&\quad\times\left[f_1(q^2)\frac{q}{m_b-m_c}+f_3(q^2)\frac{q^2}{m_b-m_c}\right]u_1(p_1,\lambda_1),\\
&\langle B_2,\lambda_2|\bar{c}\gamma_5 b|B_1,\lambda_1\rangle = \bar{u}_2(p_2,\lambda_2)\\
&\quad\times\left[-g_1(q^2)\frac{q}{m_b+m_c}-g_3(q^2)\frac{q^2}{m_b+m_c}\right]\gamma_5 u_1(p_1,\lambda_1),
\end{aligned}$$

where m_b and m_c are the respective masses of b and c quarks calculated at the renormalization scale $\mu = m_b$.

When both baryons are heavy, it is also convenient to parametrize the matrix element in the heavy quark limit, these matrix elements can be parametrized in terms of four velocities v^μ and v'^μ as follows

$$\begin{aligned}
M_\mu^V &= \langle B_2,\lambda_2|\bar{c}\gamma_\mu b|B_1,\lambda_1\rangle\\
&= \bar{u}_2(p_2,\lambda_2)[F_1(w)\gamma_\mu + F_2(w)v_\mu + F_3(w)v'_\mu]u_1(p_1,\lambda_1),\\
M_\mu^A &= \langle B_2,\lambda_2|\bar{c}\gamma_\mu\gamma_5 b|B_1,\lambda_1\rangle\\
&= \bar{u}_2(p_2,\lambda_2)[G_1(w)\gamma_\mu + G_2(w)v_\mu + G_3(w)v'^\mu]\gamma_5\\
&\quad\times u_1(p_1,\lambda_1),
\end{aligned}$$

where $w = v.v' = (M_{B_1}^2 + M_{B_2}^2 - q^2)/2M_{B_1}M_{B_2}$, M_{B_1} and M_{B_2} are the masses of the B_1 and B_2 baryons, respectively. The relationship of these two sets of form factors are related via [47]

$$\begin{aligned}
f_1(q^2) &= F_1(q^2) + (m_{B_1}+m_{B_2})\left[\frac{F_2(q^2)}{2m_{B_1}}+\frac{F_3(q^2)}{2m_{B_2}}\right],\\
f_2(q^2) &= \frac{F_2(q^2)}{2m_{B_1}}+\frac{F_3(q^2)}{2m_{B_2}},\\
f_3(q^2) &= \frac{F_2(q^2)}{2m_{B_1}}-\frac{F_3(q^2)}{2m_{B_2}},\\
g_1(q^2) &= G_1(q^2) - (m_{B_1}-m_{B_2})\left[\frac{G_2(q^2)}{2m_{B_1}}+\frac{G_3(q^2)}{2m_{B_2}}\right],\\
g_2(q^2) &= \frac{G_2(q^2)}{2m_{B_1}}+\frac{G_3(q^2)}{2m_{B_2}},\\
g_3(q^2) &= \frac{G_2(q^2)}{2m_{B_1}}-\frac{G_3(q^2)}{2m_{B_2}}.
\end{aligned} \tag{6}$$

In our numerical analysis, we follow Ref. [38] and use the form factor inputs obtained in the framework of the relativistic quark model. In the heavy quark limit, the form factors can be expressed in terms of the Isgur-Wise function $\zeta_1(w)$ as follows [38,41]

$$\begin{aligned}
F_1(w) &= G_1(w) = -\frac{1}{3}\zeta_1(w),\\
F_2(w) &= F_3(w) = \frac{2}{3}\frac{2}{w+1}\zeta_1(w),\\
G_2(w) &= G_3(w) = 0,
\end{aligned} \tag{7}$$

and the values of $\zeta_1(w)$ in the whole kinematic range, pertinent for our analysis, were mainly obtained from Ref. [38].

The helicity amplitudes can be defined by [47–51]

$$H^{V/A}_{\lambda_2,\lambda_W} = M^{V/A}_\mu(\lambda_2)\varepsilon^{\dagger\mu}(\lambda_W), \tag{8}$$

where λ_2 and λ_W denote the respective helicities of the daughter baryon and $W^-_{\text{off-shell}}$. In the rest frame of the parent baryon B_1, the vector and axial vector hadronic helicity amplitudes in the terms of the various form factors and NP coupling parameters are given by [44,47–51]

$$\begin{aligned}
H^V_{\frac{1}{2}0} &= (1+V_L+V_R)\frac{\sqrt{Q_-}}{\sqrt{q^2}}\\
&\quad\times[(M_{B_1}+M_{B_2})f_1(q^2) - q^2 f_2(q^2)],\\
H^A_{\frac{1}{2}0} &= (1+V_L-V_R)\frac{\sqrt{Q_+}}{\sqrt{q^2}}\\
&\quad\times[(M_{B_1}-M_{B_2})g_1(q^2) + q^2 g_2(q^2)],\\
H^V_{\frac{1}{2}+} &= (1+V_L+V_R)\sqrt{2Q_-}\\
&\quad\times[-f_1(q^2) + (M_{B_1}+M_{B_2})f_2(q^2)],\\
H^A_{\frac{1}{2}+} &= (1+V_L-V_R)\sqrt{2Q_+}\\
&\quad\times[-g_1(q^2) - (M_{B_1}-M_{B_2})g_2(q^2)],\\
H^V_{\frac{1}{2}t} &= (1+V_L+V_R)\frac{\sqrt{Q_+}}{\sqrt{q^2}}\\
&\quad\times[(M_{B_1}-M_{B_2})f_1(q^2) + q^2 f_3(q^2)],\\
H^A_{\frac{1}{2}t} &= (1+V_L-V_R)\frac{\sqrt{Q_-}}{\sqrt{q^2}}\\
&\quad\times[(M_{B_1}+M_{B_2})g_1(q^2) - q^2 g_3(q^2)],
\end{aligned}$$

where $Q_\pm = (M_{B_1} \pm M_{B_2})^2 - q^2$ and f_i, g_i $(i = 1, 2, 3)$ are the various form factors. Either from parity or from explicit calculation, it is clear to find that $H^V_{-\lambda_2-\lambda_W} = H^V_{\lambda_2\lambda_W}$ and $H^A_{-\lambda_2-\lambda_W} = -H^A_{\lambda_2\lambda_W}$. So the total left-handed helicity amplitude is

$$H_{\lambda_2\lambda_W} = H^V_{\lambda_2\lambda_W} - H^A_{\lambda_2\lambda_W} \tag{9}$$

Similarly, the scalar and pseudoscalar helicity amplitudes associated with the form factors and NP coupling parameters G_S and G_P can be written as

$$H^{SP}_{\lambda_2 0} = H^{S}_{\lambda_2 0} - H^{P}_{\lambda_2 0},$$
$$H^{S}_{\frac{1}{2}0} = (S_L + S_R)\frac{\sqrt{Q_+}}{m_b - m_q}[(M_{B_1} - M_{B_2})f_1(q^2) + q^2 f_3(q^2)],$$
$$H^{P}_{\frac{1}{2}0} = (S_L - S_R)\frac{\sqrt{Q_-}}{m_b + m_q}[(M_{B_1} + M_{B_2})g_1(q^2) - q^2 g_3(q^2)],$$

one can see that $H^{S}_{-\lambda_2-\lambda_W} = H^{S}_{\lambda_2\lambda_W}$ and $H^{P}_{-\lambda_2-\lambda_W} = -H^{P}_{\lambda_2\lambda_W}$. The results of above helicity amplitudes in SM can be obtained by setting $V_{L,R} = 0$ and $S_{L,R} = 0$.

B. The observables for $\Sigma_b \to \Sigma_c l\bar{\nu}_l$ and $\Omega_b \to \Omega_c l\bar{\nu}_l$

After including the NP contributions, the differential decay distribution for $\Sigma_b \to \Sigma_c l\bar{\nu}_l$ and $\Omega_b \to \Omega_c l\bar{\nu}_l$ in terms of q^2, θ_l and helicity amplitudes can be written as [47,49]

$$\frac{d^2\Gamma(B_1 \to B_2 l\bar{\nu}_l)}{dq^2 d\cos\theta_l} = N\left(1 - \frac{m_l^2}{q^2}\right)^2\left[A_1 + \frac{m_l^2}{q^2}A_2 + 2A_3 + \frac{4m_l}{\sqrt{q^2}}A_4\right], \quad (10)$$

where

$$N = \frac{G_F^2|V_{cb}|^2 q^2\sqrt{\lambda(M_{B_1}^2, M_{B_2}^2, q^2)}}{2^{10}\pi^3 M_{B_1}^3},$$
$$\lambda(a,b,c) = a^2 + b^2 + c^2 - 2(ab + bc + ca),$$
$$A_1 = 2\sin^2\theta_l(H^2_{\frac{1}{2},0} + H^2_{-\frac{1}{2},0}) + (1 - \cos\theta_l)^2 H^2_{\frac{1}{2},+} + (1 + \cos\theta_l)^2 H^2_{-\frac{1}{2},-},$$
$$A_2 = 2\cos^2\theta_l(H^2_{\frac{1}{2},0} + H^2_{-\frac{1}{2},0}) + \sin^2\theta_l(H^2_{\frac{1}{2},+} + H^2_{-\frac{1}{2},-}) + 2(H^2_{\frac{1}{2},t} + H^2_{-\frac{1}{2},t}) - 4\cos\theta_l(H_{\frac{1}{2},0}H_{\frac{1}{2},t} + H_{-\frac{1}{2},0}H_{-\frac{1}{2},t}),$$
$$A_3 = H^{SP^2}_{\frac{1}{2},0} + H^{SP^2}_{-\frac{1}{2},0},$$
$$A_4 = -\cos\theta_l(H_{\frac{1}{2},0}H^{SP}_{\frac{1}{2},0} + H_{-\frac{1}{2},0}H^{SP}_{-\frac{1}{2},0}) + (H_{\frac{1}{2},t}H^{SP}_{\frac{1}{2},0} + H_{-\frac{1}{2},t}H^{SP}_{-\frac{1}{2},0}),$$

the θ_l is the angle between the directions of the parent baryon B_1 and final lepton l three momentum vector in the dilepton rest frame.

After integrating over the $\cos\theta_l$ of Eq. (10), we can obtain the normalized differential decay rate

$$\frac{d\Gamma(B_1 \to B_2 l\bar{\nu}_l)}{dq^2} = \frac{8N}{3}\left(1 - \frac{m_l^2}{q^2}\right)^2\left[\mathcal{B}_1 + \frac{m_l^2}{2q^2}\mathcal{B}_2 + \frac{3}{2}\mathcal{B}_3 + \frac{3m_l}{\sqrt{q^2}}\mathcal{B}_4\right], \quad (11)$$

with

$$\mathcal{B}_1 = H^2_{\frac{1}{2}0} + H^2_{-\frac{1}{2}0} + H^2_{\frac{1}{2}+} + H^2_{-\frac{1}{2}-},$$
$$\mathcal{B}_2 = H^2_{\frac{1}{2}0} + H^2_{-\frac{1}{2}0} + H^2_{\frac{1}{2}+} + H^2_{-\frac{1}{2}-} + 3(H^2_{\frac{1}{2}t} + H^2_{-\frac{1}{2}t}),$$
$$\mathcal{B}_3 = (H^{SP}_{\frac{1}{2}0})^2 + (H^{SP}_{-\frac{1}{2}0})^2,$$
$$\mathcal{B}_4 = H_{\frac{1}{2}t}H^{SP}_{\frac{1}{2}0} + H_{-\frac{1}{2}t}H^{SP}_{-\frac{1}{2}0}.$$

Besides the differential decay rate, other interesting observables are also investigated and they can be written as follows:

(i) The total differential branching fraction

$$\frac{d\mathcal{B}(B_1 \to B_2 l\bar{\nu}_l)}{dq^2} = \tau_{\Omega_b(\Sigma_b)}\frac{d\Gamma(B_1 \to B_2 l\bar{\nu}_l)}{dq^2}. \quad (12)$$

(ii) The lepton side forward-backward asymmetries parameter

$$A^l_{\rm FB}(q^2) = \left(\int_{-1}^{0} d\cos\theta_l \frac{d^2\Gamma}{dq^2 d\cos\theta_l} - \int_0^1 d\cos\theta_l \frac{d^2\Gamma}{dq^2 d\cos\theta_l}\right)\Big/\frac{d\Gamma}{dq^2}. \quad (13)$$

(iii) The convexity parameter

$$C^l_F(q^2) = \frac{1}{d\Gamma/dq^2}\frac{d^2}{d(\cos\theta_l)^2}\left(\frac{d^2\Gamma}{dq^2 d\cos\theta_l}\right). \quad (14)$$

(iv) The longitudinal polarization asymmetries parameter of daughter baryons $\Omega_c(\Sigma_c)$

$$P_L^{\Omega_c(\Sigma_c)}(q^2) = \frac{{\rm d}\Gamma^{\lambda_2=1/2}/{\rm d}q^2 - {\rm d}\Gamma^{\lambda_2=-1/2}/{\rm d}q^2}{{\rm d}\Gamma/{\rm d}q^2}, \quad (15)$$

where ${\rm d}\Gamma^{\lambda_2=\pm1/2}/dq^2$ are the individual helicity dependent differential decay rates, whose detailed expressions are given in Ref. [50].

(v) The longitudinal polarization asymmetries parameter of the charged lepton

$$P_L^l(q^2) = \frac{{\rm d}\Gamma^{\lambda_l=1/2}/{\rm d}q^2 - {\rm d}\Gamma^{\lambda_l=-1/2}/{\rm d}q^2}{{\rm d}\Gamma/{\rm d}q^2}, \quad (16)$$

where ${\rm d}\Gamma^{\lambda_l=\pm1/2}/dq^2$ are differential decay rates for positive and negative helicity of lepton and their detailed expressions are also given in Ref. [50].

(vi) The ratios of the branching fractions

$${\rm R}_{\Omega_c(\Sigma_c)}(q^2) = \frac{d\mathcal{B}(B_1 \to B_2\tau\bar{\nu}_\tau)/dq^2}{d\mathcal{B}(B_1 \to B_2\ell\bar{\nu}_\ell)/dq^2}. \quad (17)$$

Note that integrating the numerator and denominator over q^2 separately before taking the ratio, we can get the average values of all the observables such as $\langle A_{\rm FB}^l \rangle$, $\langle C_F^l \rangle$, $\langle P_L^l \rangle$, $\langle P_L^{\Omega_c(\Sigma_c)} \rangle$, and $\langle {\rm R}_{\Omega_c(\Sigma_c)} \rangle$.

III. NUMERICAL ANALYSIS AND DISCUSSION

In this section, we will give our results within SM and various NP scenarios in a model independent way. We present the constrained NP coupling parameter space and give the numerical results of the observables displayed in Eqs. (12)–(17) for $\Omega_b \to \Omega_c l \bar{\nu}_l$ and $\Sigma_b \to \Sigma_c l \bar{\nu}_l$ transitions including the contributions of different NP coupling parameters. In order to get the allowed NP coupling parameter space in various NP scenarios, we will impose the 2σ constraint coming from the latest experimental values of the observables $\mathcal{B}(B \to D^{(*)} l \bar{\nu}_l)$, ${\rm R}_{D^{(*)}}$, and ${\rm R}_{J/\psi}$. The specific expressions of these observables for $B \to D^{(*)} l \bar{\nu}_l$ and $B_c \to J/\psi l \bar{\nu}_l$ processes used in our work can easily be found in the Refs. [50–54].

In our numerical computation about above various observables, except for the transition form factors and the NP coupling parameters, the values of the other input parameters such as the particle masses, decay constants, mean lives, and some relevant experimental measurement data of $\mathcal{B}(B \to D^{(*)} l \bar{\nu}_l)$ are mainly taken from the Particle Data Group (PDG) [55]. The relevant experimental data about ${\rm R}_{D^{(*)}}$ and ${\rm R}_{J/\psi}$ used in this work are listed in Eqs. (2) and (4). Note that, in the model independent analysis, we assume that all the NP coupling parameters are complex and we consider only one NP coupling existing in Eq. (5) at one time and keep it interference with the SM.

Firstly, we obtain the constrained range of NP coupling parameters V_L, V_R, S_L, and S_R by using the recent experimental measurement results, and then examine the NP effects on the observables which are displayed in Sec. II by using the constrained NP coupling parameters. The constrained the range of four NP coupling parameters V_L, V_R, S_L, and S_R are shown in the Fig. 1, and the results can be intuitively displayed by both real-imaginary and modulus-phases of the NP coupling parameters in the figure. There are few references that discuss the relationship between modulus and phases of the NP coupling parameters. The constrained results on the real, imaginary and modulus of the NP coupling parameters are listed in the Table I clearly. From Fig. 1 we can see that present experimental data give quite strong bounds on the relevant coupling parameters, in particular, modulus and phase of V_L is strongly restricted. The constrained range of V_L and S_L, V_R and S_L are shown in Fig. 2(a1-a4) and (b1-b4), respectively. From Fig. 2(a1–a4) we can see that the values of ${\rm Re}[S_L]$ and ${\rm Im}[S_L]$ are in small range compared with the values of ${\rm Re}[V_L]$ and ${\rm Im}[V_L]$. From Fig. 2(b1–b4), it is clear to find the result of V_R-S_L presents an axial symmetric phenomenon, and the scattered points are mainly distributed around the origin. Because the distribution relationship of V_L-S_R and V_R-S_R are similar to the Fig. 2, we do not show the relationship of V_L-S_R and V_R-S_R anymore.

The constraints about these NP coupling parameters obtained from various B meson decay processes have been also discussed in Refs. [1,49–51,56–58]. The NP coupling

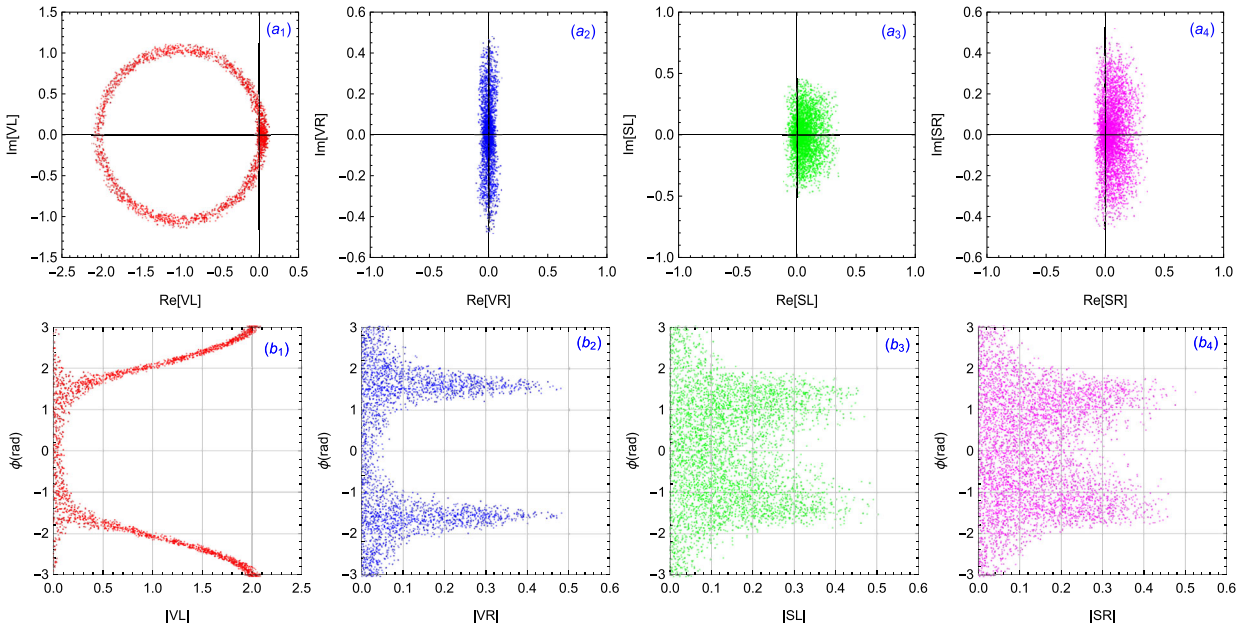

FIG. 1. The bounds on both real-imaginary (a_1-a_4) and modulus-phase (b_1-b_4) parts of the complex coupling parameters VL,VR, SL, and SR coming from the relevant experimental constraints.

TABLE I. The allowed ranges of V_L, V_R, S_L, and S_R NP coupling coefficients.

Decay mode	NP coefficients	Min value	Max value	Max of $\lvert V_i(S_i)\rvert (i = L.R)$
$b \to c l \bar{\nu}_l$	$(\mathrm{Re}[V_L], \mathrm{Im}[V_L])$	$(-2.116, -1.123)$	(0.121, 1.109)	2.118
	$(\mathrm{Re}[V_R], \mathrm{Im}[V_R])$	$(-0.105, -0.481)$	(0.105, 0.479)	0.482
	$(\mathrm{Re}[S_L], \mathrm{Im}[S_L])$	$(-0.111, -0.502)$	(0.351, 0.451)	0.502
	$(\mathrm{Re}[S_R], \mathrm{Im}[S_R])$	$(-0.094, -0.456)$	(0.355, 0.519)	0.524

parameters are assumed complex or real in these references and corresponding experimental data which are used in these references are mainly from $\mathrm{R}_{D^{(*)}}$ and $\mathrm{R}_{J/\psi}$. But few references consider the experimental data of $\mathcal{B}(B \to D^{(*)} l \bar{\nu}_l)$ which are considered in our work. In our analysis, we use the experimental data of $\mathrm{R}_{D^{(*)}}$, $\mathrm{R}_{J/\psi}$ and $\mathcal{B}(B \to D^{(*)} l \bar{\nu}_l)$ to constrain the space of the corresponding NP coupling parameters. We get more severe bounds on the phases and strengths of the NP coupling parameters and we also give the relationship between modulus and phase of four NP coupling parameters which are not discussed in many previous references.

Employing the theoretical framework described in Sec. II, the SM predictions are reported for processes $\Omega_b \to \Omega_c l \bar{\nu}_l$ and $\Sigma_b \to \Sigma_c l \bar{\nu}_l$. In Table II, we list the average values of Γ, $\langle P_L^l \rangle$, $\langle P_L^{\Omega_c(\Sigma_c)} \rangle$, $\langle A_{FB}^l \rangle$, $\langle C_F^l \rangle$, and $\langle \mathrm{R}_{\Omega_c(\Sigma_c)} \rangle$ for e, μ and τ mode respectively. From Table II, one can see that the results for e mode and μ mode are close for $\Omega_b \to \Omega_c l \bar{\nu}_l$ and $\Sigma_b \to \Sigma_c l \bar{\nu}_l$ processes. The total decay rates Γ (in units of 10^{10} s^{-1}) at $l = e$, μ are observed to be larger than the result at $l = \tau$, and same phenomenon arises in $\langle P_L^{\Omega_c(\Sigma_c)} \rangle$ and A_{FB}^l. The lepton polarization fractions P_L^l for the e and μ are negative, but one for the τ mode is positive. The forward-backward asymmetries A_{FB}^l for e and μ mode are positive, but one of the τ mode is negative. The hadron polarization fractions $P_L^{\Omega_c(\Sigma_c)}$ are about 0.58 at $l = e$, μ, and the result is about 0.35 at $l = \tau$ for both $\Omega_b \to \Omega_c l \bar{\nu}_l$ and $\Sigma_b \to \Sigma_c l \bar{\nu}_l$. All the convexity parameters $\langle C_F^l \rangle$ are negative and $\langle C_F^\tau \rangle$ is much larger than $\langle C_F^l \rangle$ $(l = e, \mu)$. The ratio of branching ratio $\langle \mathrm{R}_{\Omega_c} \rangle$ is slightly larger than $\langle \mathrm{R}_{\Sigma_c} \rangle$.

The behaviors of each observable as a function of q^2 for the processes $\Omega_b \to \Omega_c l \bar{\nu}_l$ and $\Sigma_b \to \Sigma_c l \bar{\nu}_l$ are similar to each other. So we only take $\Omega_b \to \Omega_c l \bar{\nu}_l$ decays as an example to illustrate in detail and the same goes in the following text. The SM predictions for the q^2 dependency of different observables in the reasonable kinematic range for $\Omega_b \to \Omega_c l \bar{\nu}_l$ are displayed in Fig. 3. In this figure, we compare the distributions of the each observable and the red dot dash line, blue and green line represents the e, μ and τ mode, respectively. The q^2 dependency of $d\Gamma/dq^2$, A_{FB}^l, C_F^l, and P_L^l are distinct for three generation leptons. But we can find that the variation tendency of $d\Gamma/dq^2$, A_{FB}^l, C_F^l, and P_L^l for e and μ modes is almost same except in small q^2

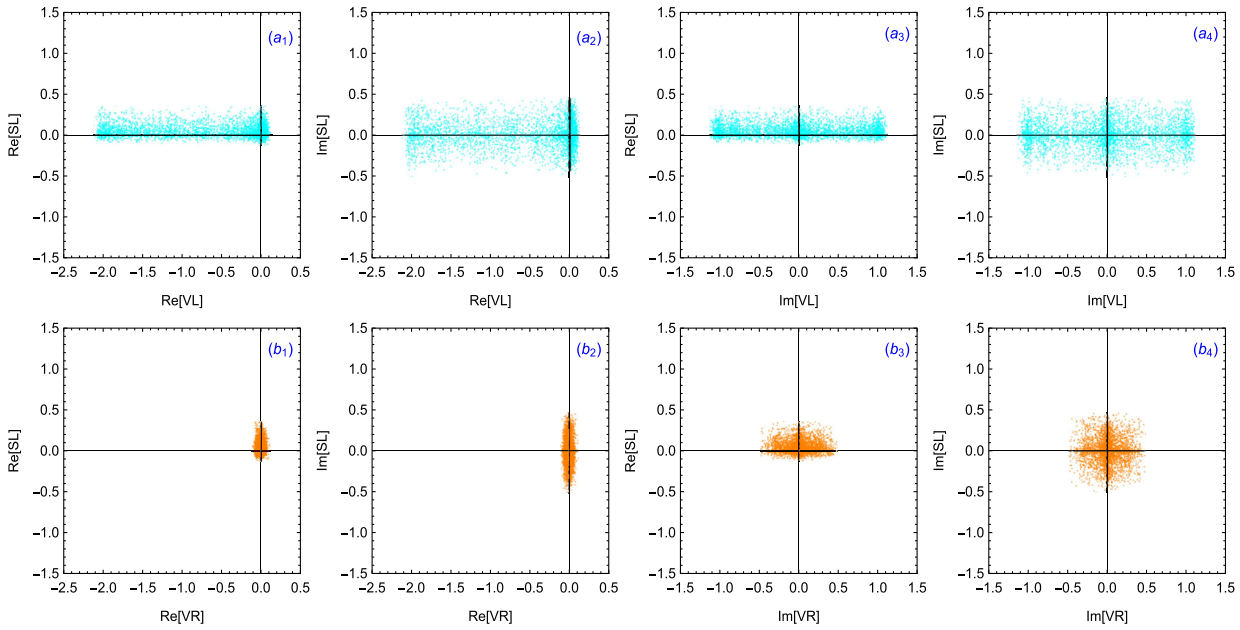

FIG. 2. The bounds on both real and imaginary parts of the complex coupling parameters VL and SL (a_1-a_4), VR and SL (b_1-b_4) coming from the relevant experimental results.

TABLE II. The SM central values for the decay rate Γ, the lepton polarization fraction $\langle P_L^l \rangle$, the hadron polarization fraction $\langle P_L^{\Sigma_c(\Omega_c)} \rangle$, the forward-backward asymmetry $\langle A_{FB}^l \rangle$, the convexity factor $\langle C_F^l \rangle$, and the ratio of branching ratio $\langle R_{\Sigma_c(\Omega_c)} \rangle$ for the e mode, μ mode, and τ mode of $\Omega_b \to \Omega_c l \bar{\nu}_l$ and $\Sigma_b \to \Sigma_c l \bar{\nu}_l$ decays.

	$\Omega_b \to \Omega_c l\nu$			$\Sigma_b \to \Sigma_c l\nu$		
	e mode	μ mode	τ mode	e mode	μ mode	τ mode
$\Gamma \times 10^{10}$ s^{-1}	1.295	1.292	0.529	1.610	1.641	0.540
$\langle P_L^l \rangle$	−1.123	−1.093	0.135	−1.135	−1.131	0.132
$\langle P_L^{\Omega_c(\Sigma_c)} \rangle$	0.586	0.585	0.354	0.582	0.582	0.355
$\langle A_{FB}^l \rangle$	0.062	0.052	−0.220	0.065	0.055	−0.220
$\langle C_F^l \rangle$	−1.170	−1.140	−0.135	−1.178	−1.148	−0.139
$\langle R_{\Omega_c(\Sigma_c)} \rangle$		$R_{\Omega_c} = 0.370$			$R_{\Sigma_c} = 0.339$	

region. The total differential decay rate for e is maximum at $q^2_{\rm min}$ and minimum at $q^2_{\rm max}$, however, the result for τ is maximum when $q^2 \approx 8$ GeV^2 and approaches zero at $q^2_{\rm min}$ and $q^2_{\rm max}$. For μ mode, $d\Gamma/dq^2$ changes to zero quickly when $q^2 = m_\mu^2$ due to the effect of μ mass. All the A_{FB}^l approach to zero at $q^2_{\rm max}$. The A_{FB}^e is positive while A_{FB}^τ is negative and great increasing with q^2 over the all q^2 region. Besides, A_{FB}^μ changes to -0.4 quickly when $q^2 = m_\mu^2$ and there is a zero-crossing point, which lies in the low q^2 region. All the C_F^l are negative in the whole q^2 region and at the large q^2 limit C_F^l are zero. At the low q^2 range C_F^e is around -1.5 when $q^2 = q^2_{\rm min}$, and $C_F^\mu \approx -1.4$ when $q^2 \approx 0.4$ GeV^2, while C_F^μ changes to zero quickly when $q^2 = m_\mu^2$ due to the effect of the lepton mass. This behavior indicates that the $\cos\theta$ distribution in $q^2 \in [0.4, 11.23]$ is strongly parabolic. On the contrary, the C_F^τ is small in the whole ranges, which implies a straight line behavior of the $\cos\theta$ distribution. The $P_L^{\Omega_c}$ are zero for three modes at $q^2_{\rm max}$. The results of $P_L^{\Omega_c}$ for e and μ modes completely coincide and it is around 0.6 at $q^2 = q^2_{\rm min} = m_l^2$. The P_L^e is -1 over the all q^2 region and it is similar to μ mode except for low q^2 region. When $q^2 = m_\mu^2$, the P_L^μ changes to 0.4 quickly. While for the τ mode, the behavior is quite different and P_L^τ take only positive values for entire q^2 values. The R_{Ω_c} show

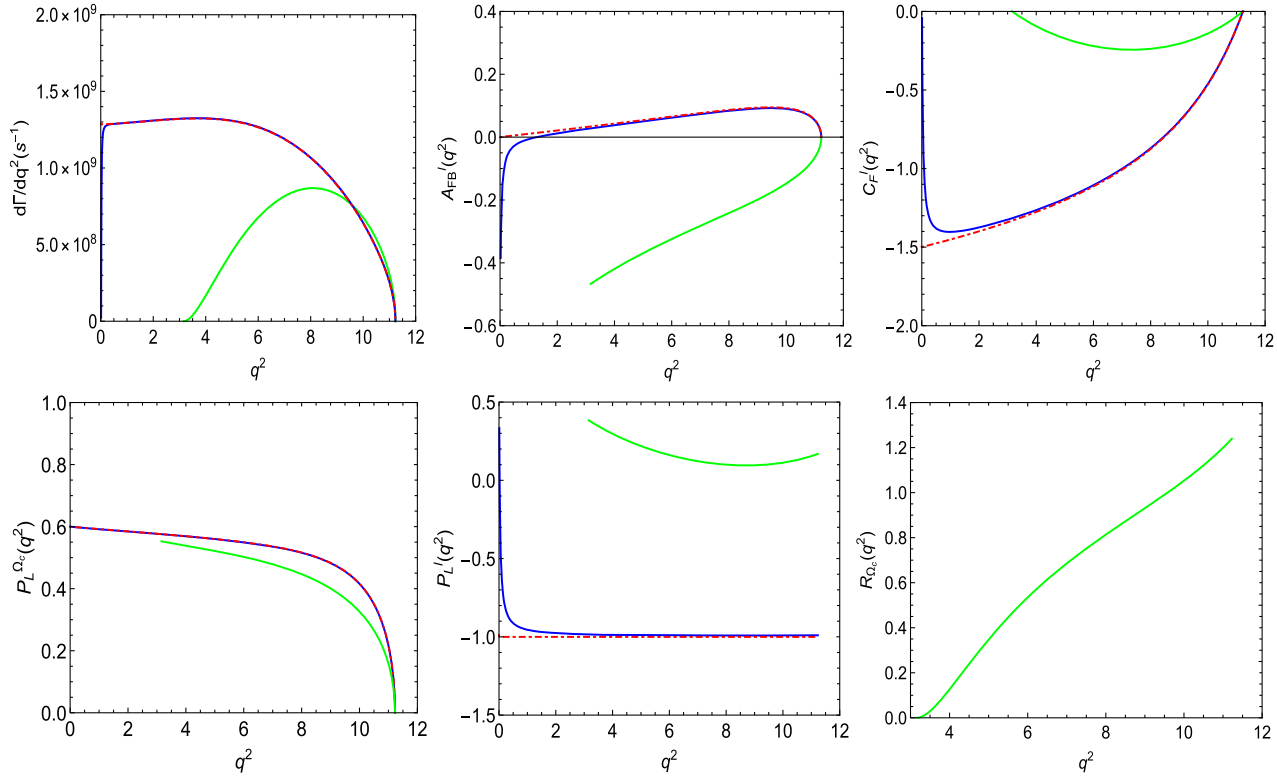

FIG. 3. The SM predictions for the q^2 dependent observables $d\Gamma/dq^2$, $A_{FB}^l(q^2)$, $C_F^l(q^2)$, $P_L^{\Omega_c}(q^2)$, $P_L^l(q^2)$, and $R_{\Omega_c}(q^2)$ relative to the decays $\Omega_b \to \Omega_c l \bar{\nu}_l$ ($\ell = e, \mu, \tau$). The red dot dash line, blue, and green line represent the e, μ and τ mode, respectively.

an almost positive slope over the whole q^2 region and R_{Ω_c} is around 0 when $q^2 = q^2_{\min}$. Because the R_{Ω_c} is ratios of the differential branching fraction with the heavier τ in the final state to the differential branching fraction with the lighter lepton in the final state, the result of this observable do not distinguish for the different leptons in the final state.

Next, we proceed to investigate the effects of these four NP coupling parameters V_L, V_R, S_L, and S_R on the above observables for various NP scenarios in a model independent way. In order to avoid repetition, we only display the q^2 dependency of each observable for decay $\Omega_b \to \Omega_c \tau \bar{\nu}_\tau$ and the results are displayed in Fig. 4. In the figure we report the q^2 dependency of the observables $d\Gamma/dq^2$,

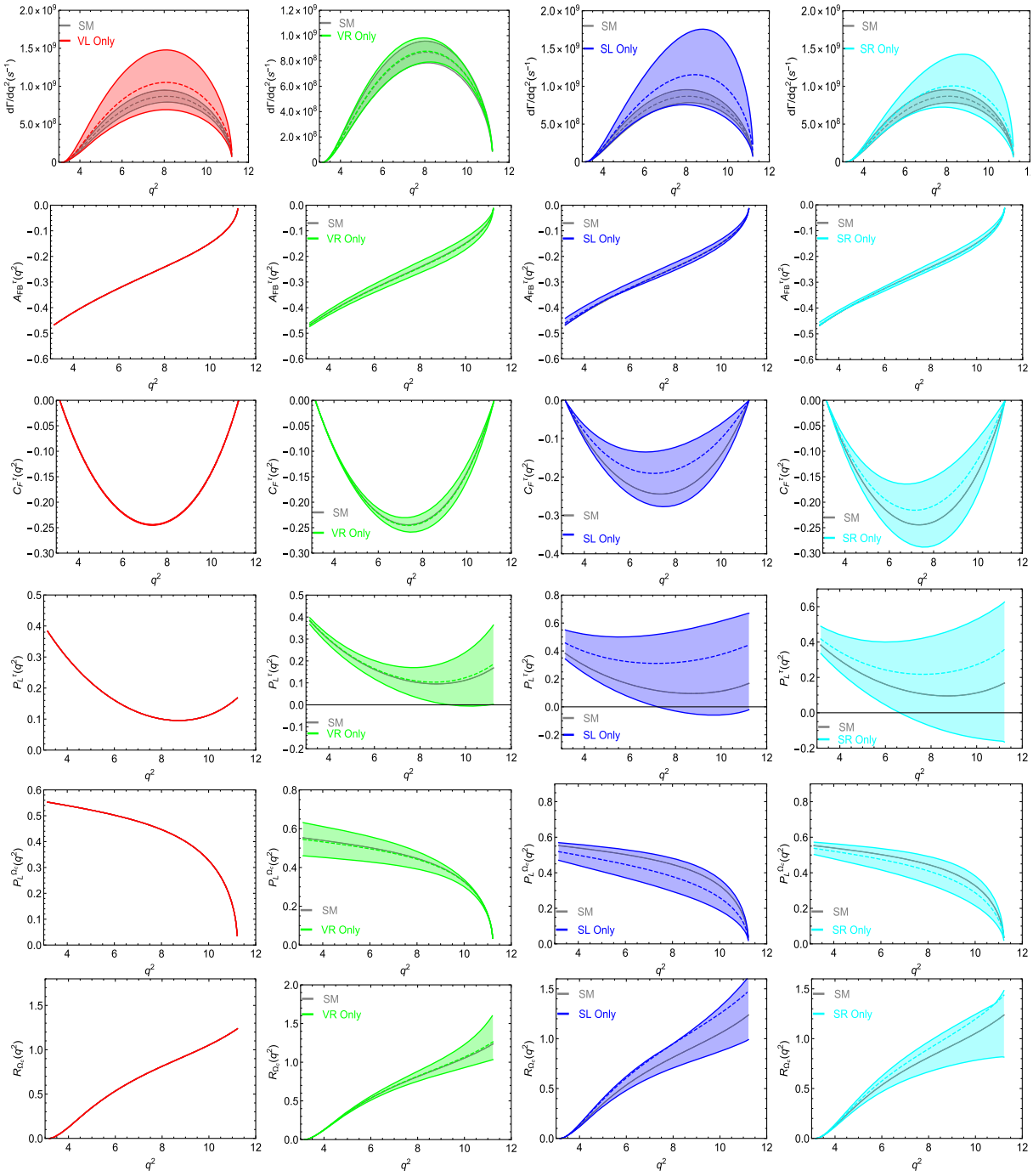

FIG. 4. The SM (gray) and NP predictions in the presence of V_L (first column), V_R (second column), S_L (third column), and S_R (fourth column) coupling for the q^2 dependency observables $d\Gamma/dq^2$, $A^{\tau}_{FB}(q^2)$, $C^{\tau}_F(q^2)$, $P^{\tau}_L(q^2)$, $P^{\Omega_c}_L(q^2)$, and $R_{\Omega_c}(q^2)$ relative to the decay $\Omega_b \to \Omega_c \tau \bar{\nu}_\tau$.

$A_{FB}^{\tau}(q^2)$, $C_F^{\tau}(q^2)$, $P_L^{\tau}(q^2)$, $P_L^{\Omega_c}(q^2)$ and $\mathrm{R}_{\Omega_c}(q^2)$ for $\Omega_b \to \Omega_c \tau \bar{\nu}_\tau$ transition including the contribution of only one NP vector or scalar type coupling parameter, and we incorporate both SM and NP result. In the Fig. 4, the band for the input parameters (form factors and V_{cb}) and different NP coupling parameters restricted by the relative experimental values of the processes $B \to D^{(*)} l \bar{\nu}_l$ and $B_c \to J/\psi l \bar{\nu}_l$ are represented with that different colors. The SM and four NP scenarios are distinguished by gray (SM), red (V_L), green (V_R), blue (S_L), and cyan (S_R) colors, respectively. In the Fig. 4, we suppose that the NP contributions only come from one NP coupling and we find the following remarks:

(i) When we only consider the effect of vector NP coupling V_L, the effect of this NP coupling appears in the $H^V_{\lambda_2,\lambda_W}$ and $H^A_{\lambda_2,\lambda_W}$ only. From Eq. (11), it is clear to find that the $d\Gamma/dq^2$ depends on $(1+V_L)^2$ only. Using the constrained range of V_L which are displayed in the Fig. 1, one can see that the deviation from the SM prediction due to the V_L coupling is observed only in the total differential decay rate $d\Gamma/dq^2$ and the observable is proportional to $(1+V_L)^2$. The $d\Gamma/dq^2$ is largely enhanced in the whole q^2 region. Moreover, the factor $(1+V_L)^2$ appears both in the numerator and denominator of the expressions which describe other observables simultaneously. So the NP dependency cancels in the ratios and we do not see any deviation from the SM prediction for other observables.

(ii) Similar to V_L, the NP coupling parameter V_R is also included in the vector and the axial-vector helicity amplitudes. In this case, the $d\Gamma/dq^2$ depends on both $(1+V_R)^2$ and $(1-V_R)^2$. Hence, there is no cancellation of NP effects in the ratios and there is deviation in each observable from the SM prediction. The deviation of $d\Gamma/dq^2$ from their SM prediction is not so significant, while, it is very significant for other observables. The effects of the V_R coupling are rather significant on the observables $P_L^{\tau}(q^2)$, $P_L^{\Omega_c}(q^2)$, and $\mathrm{R}_{\Omega_c}(q^2)$, especially in largest q^2 region for $P_L^{\tau}(q^2)$ and $\mathrm{R}_{\Omega_c}(q^2)$ and lowest q^2 region for $P_L^{\Omega_c}(q^2)$.

(iii) The effects of the scalar NP coupling S_L come into the scalar and pseudoscalar helicity amplitudes $H^S_{\lambda_2,\lambda_W}$ and $H^P_{\lambda_2,\lambda_W}$. One can see that it is different from V_L and V_R coupling scenarios. From Eq. (11) one can see that $d\Gamma/dq^2$ depends on S_L and S_L^2 in this case. So there is also no cancellation in the numerator and denominator of the expressions in other observables simultaneously. We can find that the deviation from their SM prediction is more pronounced than that with V_L and V_R NP coupling except $A_{FB}^{\tau}(q^2)$. The deviation from the SM prediction for $d\Gamma/dq^2$ is most prominent at $q^2 \approx 8.8\ \mathrm{GeV}^2$. When consider the value of the S_L NP coupling, there may or may not be a zero crossing in the $P_L^{\tau}(q^2)$, while there is no zero crossing for $P_L^{\tau}(q^2)$ in the SM prediction. Besides, the deviations from their SM prediction for $P_L^{\tau}(q^2)$ and $\mathrm{R}_{\Omega_c}(q^2)$ are most prominent at largest q^2 region. There are some differences between our results and Ref. [44] for S_L NP coupling scenario. In Ref. [44], there are two constraint results for S_L NP coupling and they are $S_L \in [-0.2, 0.1]$ and $[-1.6, -1.4]$ respectively. The authors use $S_L \in [-1.6, -1.4]$ when considering the NP effect of S_L. If $S_L \in [-0.2, 0.1]$ in their analysis, their result are similar to our work for this scenario.

(iv) From last column in Fig. 4 considering the S_R NP coupling, the change trend of each observable are similar to the S_L scenario. Because NP effects which come from the S_R NP coupling are also encoded in the scalar and pseudoscalar helicity amplitudes only, the $d\Gamma/dq^2$ depends on S_R and S_R^2. The deviation from the SM prediction of $d\Gamma/dq^2$ may be less obvious than the S_L scenario. However, it is larger for $C_F^{\tau}(q^2)$ compared to S_L scenario. In the $P_L^{\tau}(q^2)$, the zero -crossing point may shift slightly toward a lower q^2 value than in the S_L case.

Finally, we also explore the impact of these four combinations for vector and scalar type couplings such as V_L-S_L, V_L-S_R, V_R-S_L, and V_R-S_R to above various observables for $\Omega_b \to \Omega_c \tau \bar{\nu}_\tau$ process. We find that the NP predictions of the same observables in these four combinations NP scenarios show a similar variation tendency to the increasing of q^2 and have similar deviations to their corresponding S_L and S_R predictions, except that the value of the corresponding longitudinal axis is different. In order to avoid repetition, we do not display the results of different combinations anymore. At the same time we find that similar conclusions can be also made for the $\Sigma_b \to \Sigma_c \tau \bar{\nu}_\tau$ decay process.

IV. SUMMARY

Several anomalies $\mathrm{R}_{D^{(*)}}$ and $\mathrm{R}_{J/\psi}$ observed in the semileptonic B meson decays have indicated the hints of LFUV and attracted the attention of many researchers. Many works about baryon decays $\Lambda_b \to \Lambda_c(p) l \bar{\nu}_l$ and $\Xi_b \to \Xi_c(\Lambda) l \bar{\nu}_l$ have been done to investigate the NP effects of above anomalies on the precess $b \to c(u) l \bar{\nu}_l$. These baryon decays not only can provide an independent determination of the CKM matrix element $|V_{cb}|$ but also may be further confirmation of the hints of LFUV that is helpful in exploring NP. At present, there exist few quantitative measurement for the semileptonic decay of Ω_b and Σ_b due the complexity baryons structures and the lack of precise predictions of various form factors. It is indeed necessary to investigate the semileptonic baryon decays $\Omega_b \to \Omega_c l \bar{\nu}_l$ and $\Sigma_b \to \Sigma_c l \bar{\nu}_l$ both theoretically and experimentally to test the LFUV.

In this work we have used the helicity formalism to get various angular decay distribution and have performed a model independent analysis of baryonic $\Omega_b \to \Omega_c l\bar{\nu}_l$ and $\Sigma_b \to \Sigma_c l\bar{\nu}_l$ decay processes. In this work we considered the NP coupling parameters to be complex in our analysis. In order to constrain the various NP coupling parameters, we have assumed that only one NP coupling parameter is present one time. We have gotten strong bounds on the phases and strengths of the various NP coupling parameters from the latest experimental limits of $B \to D^{(*)} l\bar{\nu}_l$ and $B_c \to J/\psi l\bar{\nu}_l$. Using the constrained NP coupling parameters, we have estimated various observables of the $\Omega_b \to \Omega_c l\bar{\nu}_l$ and $\Sigma_b \to \Sigma_c l\bar{\nu}_l$ baryon decays in the SM and various NP scenarios in a model independent way. The numerical results have been presented for e, μ, and τ mode respectively in SM. We also display the q^2 dependency of different observables for $\Omega_b \to \Omega_c \tau\bar{\nu}_\tau$ process within the SM and various NP coupling scenarios. The results show that $d\Gamma/dq^2$ including any kind of NP couplings are all enhanced largely and have significant deviations comparing to their SM predictions in whole q^2 region. In the V_L scenario, the observables $A_{FB}^{\tau}(q^2)$, $C_F^{\tau}(q^2)$, $P_L^{\tau}(q^2)$, $P_L^{\Omega_c(\Sigma_c)}(q^2)$, and $\mathrm{R}_{\Omega_c(\Sigma_c)}(q^2)$ are the same as their corresponding SM predictions because the coefficient $(1+V_L)^2$ appears in the numerator and the denominator of the expressions which describing these observables simultaneously. We noticed a profound deviation in all angular observables of the semileptonic baryonic $b \to c\tau\bar{\nu}_\tau$ process due to the additional contribution of V_R, S_L and S_R couplings to the SM. The deviations from their SM prediction of $P_L^{\tau}(q^2)$ and $\mathrm{R}_{\Omega_c}(q^2)$ are most prominent at largest q^2 region.

Until now there are only some experimental data about the nonleptonic decay of Ω_b and Σ_b, and there is poor quantitative measurement of the semileptonic decay rates of Ω_b and Σ_b, Though there is no experimental measurement on these baryonic $b \to c l\bar{\nu}_l$ decay processes, the study of this work is found to be very crucial in order to shed light on the nature of NP. In the near future, more data on Ω_b will be obtained by the LHCb experiments and we hope the results of the observables discussed in this work can be tested at experimental facilities at BEPCII, LHCb, and Belle II.

ACKNOWLEDGMENTS

We would like to thank Yuan-Guo Xu for providing us some helpful discussion and constant encouragement on the manuscript. This work was supported by the National Natural Science Foundation of China (Contracts No. 11675137 and No. 11947083) and the Key Scientific Research Projects of Colleges and Universities in Henan Province (Contract No. 18A140029).

[1] A. Ray, S. Sahoo, and R. Mohanta, Model independent analysis of $B^* \to P\ell\bar{\nu}_\ell$ decay processes, Eur. Phys. J. C **79**, 670 (2019).

[2] Q. Chang, J. Zhu, X. L. Wang, J. F. Sun, and Y. L. Yang, Study of semileptonic $B^* \to Pl\bar{\nu}_l$ decays, Nucl. Phys. **B909**, 921 (2016).

[3] Y. Li and C. D. Lü, Recent anomalies in B physics, Sci. Bull. **63**, 267 (2018).

[4] S. Bifani, S. Descotes-Genon, A. Romero Vidal, and M. H. Schune, Review of lepton universality tests in B decays, J. Phys. G **46**, 023001 (2019).

[5] J. Lees *et al.* (BABAR Collaboration), Evidence for an Excess of $\bar{B} \to D^{(*)}\tau^-\bar{\nu}_\tau$ Decays, Phys. Rev. Lett. **109**, 101802 (2012).

[6] M. Huschle *et al.* (Belle Collaboration), Measurement of the branching ratio of $\bar{B} \to D^{(*)}\tau^-\bar{\nu}_\tau$ relative to $\bar{B} \to D^{(*)}\ell^-\bar{\nu}_\ell$ decays with hadronic tagging at Belle, Phys. Rev. D **92**, 072014 (2015).

[7] A. Abdesselam *et al.* (Belle Collaboration), Measurement of the branching ratio of $\overline{B}^0 \to D^{*+}\tau^-\bar{\nu}_\tau$ relative to $\bar{B}^0 \to D^{*+}l\bar{\nu}_l$ decays with a semileptonic tagging method, arXiv: 1603.06711.

[8] A. Abdesselam *et al.* (Belle Collaboration), Measurement of the τ lepton polarization in the decay $\bar{B} \to D^*\tau\bar{\nu}_\tau$, arXiv: 1608.06391.

[9] R. Aaij *et al.* (LHCb Collaboration), Measurement of the Ratio of Branching Fractions $\mathcal{B}(\bar{B}^0 \to D^{*+}\tau^-\bar{\nu}_\tau)/\mathcal{B}(\bar{B}^0 \to D^{*+}\mu^-\bar{\nu}_\mu)$, Phys. Rev. Lett. **115**, 111803 (2015).

[10] R. Aaij *et al.* (LHCb Collaboration), Measurement of the Ratio of the $B^0 \to D^{*-}\tau^+\nu_\tau$ and $B^0 \to D^{*-}\mu^+\nu_\mu$ Branching Fractions Using Three-Prong τ-Lepton Decays, Phys. Rev. Lett. **120**, 171802 (2018).

[11] A. Abdesselam *et al.* (Belle), Measurement of $\mathcal{R}(D)$ and $\mathcal{R}(D^*)$ with a semileptonic tagging method, arXiv: 1904.08794.

[12] HFLAV Collaboration, Online update for averages of R_D and R_{D^*} for Spring 2019 at https://hflav-eos.web.cern.ch/hflav-eos/semi/spring19/html/RDsDsstar/RDRDs.html.

[13] R. Aaij *et al.* (LHCb Collaboration), Measurement of the Ratio of Branching Fractions $\mathcal{B}(B_c^+ \to J/\psi\tau^+\nu_\tau)/\mathcal{B}(B_c^+ \to J/\psi\mu^+\nu_\mu)$, Phys. Rev. Lett. **120**, 121801 (2018).

[14] R. Dutta and A. Bhol, $B_c \to (J/\psi, \eta_c)\tau\nu$ semileptonic decays within the standard model and beyond, Phys. Rev. D **96**, 076001 (2017).

[15] W. F. Wang, Y. Y. Fan, and Z. J. Xiao, Semileptonic decays $B_c \to (\eta_c, J/\Psi)l\nu$ in the perturbative QCD approach, Chin. Phys. C **37**, 093102 (2013).

[16] X. Q. Hu, S. P. Jin, and Z. J. Xiao, Semileptonic decays $B_c \to (\eta_c, J/\psi)l\bar{\nu}_l$ in the "PQCD + Lattice" approach, Chin. Phys. C **44**, 023104 (2020).

[17] R. Watanabe, New physics effect on $B_c \to J/\psi\tau\bar{\nu}$ in relation to the $R_{D^{(*)}}$ anomaly, Phys. Lett. B **776**, 5 (2018).

[18] W. Wang and R. Zhu, Model independent investigation of the $R_{J/\psi,\eta_c}$ and ratios of decay widths of semileptonic B_c decays into a P-wave charmonium, Int. J. Mod. Phys. A **34**, 1950195 (2019).

[19] Y. Sakaki, M. Tanaka, A. Tayduganov, and R. Watanabe, Probing new physics with q^2 distributions in $\bar{B} \to D^{(*)}\tau\bar{\nu}$, Phys. Rev. D **91**, 114028 (2015).

[20] S. Bhattacharya, S. Nandi, and S. K. Patra, Looking for possible new physics in $B \to D^{(*)}\tau\nu_\tau$ in light of recent data, Phys. Rev. D **95**, 075012 (2017).

[21] F. Feruglio, P. Paradisi, and O. Sumensari, Implications of scalar and tensor explanations of $R_{D^{(*)}}$, J. High Energy Phys. 11 (2018) 191.

[22] M. Jung and D. M. Straub, Constraining new physics in $b \to c l\bar{\nu}_l$ transitions, J. High Energy Phys. 01 (2019) 009.

[23] Q.-Y. Hu, X.-Q. Li, and Y.-D. Yang, $b \to c\tau\nu$ transitions in the standard model effective field theory, Eur. Phys. J. C **79**, 264 (2019).

[24] X. L. Mu, Y. Li, Z. T. Zou, and B. Zhu, Investigation of effects of new physics in $\Lambda_b \to \Lambda_c\tau\bar{\nu}_\tau$ decay, Phys. Rev. D **100**, 113004 (2019).

[25] Z. R. Huang, Y. Li, C. D. Lu, M. A. Paracha, and C. Wang, Footprints of new physics in $b \to c\tau\nu$ transitions, Phys. Rev. D **98**, 095018 (2018).

[26] X. Q. Li, Y. D. Yang, and X. Zhang, Revisiting the one leptoquark solution to the $R(\mathrm{D}^{(*)})$ anomalies and its phenomenological implications, J. High Energy Phys. 08 (2016) 054.

[27] H. Yan, Y. D. Yang, and X. B. Yuan, Phenomenology of $b \to c\tau\bar{\nu}$ decays in a scalar leptoquark model, Chin. Phys. C **43**, 083105 (2019).

[28] R. Barbieri, C. W. Murphy, and F. Senia, B-decay anomalies in a composite leptoquark model, Eur. Phys. J. C **77**, 8 (2017).

[29] Q.-Y. Hu, X.-Q. Li, Y. Muramatsu, and Y.-D. Yang, R-parity violating solutions to the $R_{D^{(*)}}$ anomaly and their GUT-scale unifications, Phys. Rev. D **99**, 015008 (2019).

[30] Q.-Y. Hu, Y.-D. Yang, and M.-D. Zheng, Revisiting the B-physics anomalies in R-parity violating MSSM, Eur. Phys. J. C **80**, 365 (2020).

[31] C. H. Chen and T. Nomura, Charged-Higgs on $R_{D^{(*)}}$, τ polarization, and FBA, Eur. Phys. J. C **77**, 631 (2017).

[32] S. Iguro and K. Tobe, $R_{D^{(*)}}$ in a general two Higgs doublet model, Nucl. Phys. **B925**, 560 (2017).

[33] M. Tanaka and R. Watanabe, Tau longitudinal polarization in $B \to D\tau\nu_\tau$ and its role in the search for charged Higgs boson, Phys. Rev. D **82**, 034027 (2010).

[34] S. Matsuzaki, K. Nishiwaki, and R. Watanabe, Phenomenology of flavorful composite vector bosons in light of B anomalies, J. High Energy Phys. 08 (2017) 145.

[35] H. Park *et al.* (HyperCP Collaboration), Evidence for the Decay $\Sigma^+ \to p\mu^+\mu^-$, Phys. Rev. Lett. **94**, 021801 (2005).

[36] M. A. Ivanov, J. G. Korner, V. E. Lyubovitskij, and A. G. Rusetsky, Charm and bottom baryon decays in the Bethe-Salpeter approach: Heavy to heavy semileptonic transitions, Phys. Rev. D **59**, 074016 (1999).

[37] M. A. Ivanov, V. E. Lyubovitskij, J. G. Korner, and P. Kroll, Heavy baryon transitions in a relativistic three quark model, Phys. Rev. D **56**, 348 (1997).

[38] D. Ebert, R. N. Faustov, and V. O. Galkin, Semileptonic decays of heavy baryons in the relativistic quark model, Phys. Rev. D **73**, 094002 (2006).

[39] R. L. Singleton, Semileptonic baryon decays with a heavy quark, Phys. Rev. D **43**, 2939 (1991).

[40] H. W. Ke, N. Hao, and X. Q. Li, Revisiting $\Lambda_b \to \Lambda_c$ and $\Sigma_b \to \Sigma_c$ weak decays in the light-front quark model, Eur. Phys. J. C **79**, 540 (2019).

[41] H. W. Ke, X. H. Yuan, X. Q. Li, Z. T. Wei, and Y. X. Zhang, $\Sigma_b \to \Sigma_c$ and $\Omega_b \to \Omega_c$ weak decays in the light-front quark model, Phys. Rev. D **86**, 114005 (2012).

[42] H. W. Ke, N. Hao, and X. Q. Li, $\Sigma_b \to \Sigma_c^*$ weak decays in the light-front quark model with two schemes to deal with the polarization of diquark, J. Phys. G **46**, 115003 (2019).

[43] M. k. Du and C. Liu, Ω_b semi-leptonic weak decays, Phys. Rev. D **84**, 056007 (2011).

[44] N. Rajeev, R. Dutta, and S. Kumbhakar, Implication of $R_{D^{(*)}}$ anomalies on semileptonic decays of Σ_b and Ω_b baryons, Phys. Rev. D **100**, 035015 (2019).

[45] V. Cirigliano, J. Jenkins, and M. Gonzalez-Alonso, Semileptonic decays of light quarks beyond the Standard Model, Nucl. Phys. **B830**, 95 (2010).

[46] T. Bhattacharya, V. Cirigliano, S. D. Cohen, A. Filipuzzi, M. Gonzalez Alonso, M. L. Graesser, R. Gupta, and H. W. Lin, Probing novel scalar and tensor interactions from (ultra) cold neutrons to the LHC, Phys. Rev. D **85**, 054512 (2012).

[47] R. Dutta, Phenomenology of $\Xi_b \to \Xi_c\tau\nu$ decays, Phys. Rev. D **97**, 073004 (2018).

[48] T. Gutsche, M. A. Ivanov, J. G. Korner, V. E. Lyubovitskij, P. Santorelli, and N. Habyl, Semileptonic decay $\Lambda_b \to \Lambda_c\tau^-\bar{\nu}_\tau$ in the covariant confined quark model, Phys. Rev. D **91**, 074001 (2015).

[49] S. Shivashankara, W. Wu, and A. Datta, $\Lambda_b \to \Lambda_c\tau\bar{\nu}_\tau$ Decay in the Standard Model and with new physics, Phys. Rev. D **91**, 115003 (2015).

[50] A. Ray, S. Sahoo, and R. Mohanta, Probing new physics in semileptonic Λ_b decays, Phys. Rev. D **99**, 015015 (2019).

[51] J. Zhang, X. An, R. Sun, and J. Su, Probing new physics in semileptonic $\Xi_b \to \Lambda(\Xi_c)\tau^-\bar{\nu}_\tau$ decays, Eur. Phys. J. C **79**, 863 (2019).

[52] R. Dutta, A. Bhol, and A. K. Giri, Effective theory approach to new physics in $b \to u$ and $b \to c$ leptonic and semileptonic decays, Phys. Rev. D **88**, 114023 (2013).

[53] Y. Sakaki, M. Tanaka, A. Tayduganov, and R. Watanabe, Testing leptoquark models in $\bar{B} \to D^{(*)}\tau\bar{\nu}$, Phys. Rev. D **88**, 094012 (2013).

[54] R. Dutta and A. Bhol, $b \to (c, u), \tau\nu$ leptonic and semileptonic decays within an effective field theory approach, Phys. Rev. D **96**, 036012 (2017).

[55] P. A. Zyla *et al.* (Particle Data Group), Review of particle physics, Prog. Theor. Exp. Phys. **2020**, 083C01 (2020).

[56] M. A. Ivanov, J. G. Korner, and C. T. Tran, Analyzing new physics in the decays $\bar{B}^0 \to D^{(*)}\tau^-\bar{\nu}_\tau$ with form factors

obtained from the covariant quark model, Phys. Rev. D **94**, 094028 (2016).

[57] M. A. Ivanov, J. G. Korner, and C. T. Tran, Probing new physics in $\bar{B}^0 \to D^{(*)}\tau^-\bar{\nu}_\tau$ using the longitudinal, transverse, and normal polarization components of the tau lepton, Phys. Rev. D **95**, 036021 (2017).

[58] R. Dutta, $\Lambda_b \to (\Lambda_c, p)\tau\nu$ decays within standard model and beyond, Phys. Rev. D **93**, 054003 (2016).